Water Research 256 (2024) 121618

Contents lists available at ScienceDirect

Water Research

journal homepage: www.elsevier.com/locate/watres

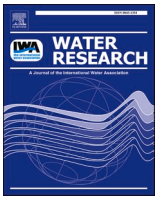

# Advancing towards electro-bioremediation scaling-up: *On-site* pilot plant for successful nitrate-contaminated groundwater treatment

Alba Ceballos-Escalera [a], Narcís Pous [a], Lluis Bañeras [b], M. Dolors Balaguer [a], Sebastià Puig [a,*]

[a] LEQUiA, Institute of the Environment, University of Girona, C/ Maria Aurèlia Capmany, 69, E-17003, Girona, Spain
[b] Group of Environmental Microbial Ecology, Institute of Aquatic Ecology, University of Girona, C/ Maria Aurèlia Capmany, 40, E-17003, Girona, Spain

ARTICLE INFO

*Keywords:*
Microbial electrochemical technology
Bioelectrochemical system
Biological denitrification
Decentralised water treatment
Groundwater

ABSTRACT

The potential of nitrate electro-bioremediation has been fully demonstrated at the laboratory scale, although it has not yet been fully implemented due to the challenges associated with scaling-up bioelectrochemical reactors and their on-site operation. This study describes the initial start-up and subsequent stable operation of an electro-bioremediation pilot plant for the treatment of nitrate-contaminated groundwater *on-site* (Navata site, Spain). The pilot plant was operated under continuous flow mode for 3 months, producing an effluent suitable for drinking water in terms of nitrates and nitrites (<50 mg $NO_3^-$ $L^{-1}$; 0 mg $NO_2^-$ $L^{-1}$). A maximum nitrate removal rate of 0.9 ± 0.1 kg $NO_3^-$ $m^{-3}$ $d^{-1}$ (efficiency 82 ± 18 %) was achieved at a cathodic hydraulic retention time ($HRT_{cat}$) of 2.0 h with a competitive energy consumption of 4.3 ± 0.4 kWh $kg^{-1}$ $NO_3^-$. Under these conditions, the techno-economic analysis estimated an operational cost of 0.40 € $m^{-3}$. Simultaneously, microbiological analyses revealed structural heterogeneity in the reactor, with denitrification functionality concentrated predominantly from the centre to the upper section of the reactor. The most abundant groups were *Pseudomonadaceae, Rhizobiaceae, Gallionellaceae*, and *Xanthomonadaceae*. In conclusion, this pilot plant represents a significant advancement in implementing this technology on a larger scale, validating its effectiveness in terms of nitrate removal and cost-effectiveness. Moreover, the results validate the electro-bioremediation in a real environment and encourage further investigation of its potential as a water treatment.

## 1. Introduction

Water pollution affects around 40 % of freshwater reserves, and it has become a global threat (U.N. Water, 2021). It exacerbates water stress and negatively impacts environmental sustainability, economic stability and human health. In particular, groundwater in rural areas is highly vulnerable to pollution from intensive agricultural and livestock farming practices, resulting in around 18 % of groundwater bodies in Europe being contaminated with nitrates in 2018 (EEA et al., 2018). Given the global concern over nitrate contamination due to its associated health risks, the European Directive 2020/2184 sets a nitrate concentration limit of 50.0 mg $NO_3^-$ $L^{-1}$ and 0.5 mg $NO_2^-$ $L^{-1}$ to ensure the safety of drinking water. However, the water services management to ensure water quality and safety in rural areas remains limited, with only around 60 % coverage (WHO, 2021). This is primarily due to the high cost and extensive infrastructure required for conventional centralised treatments, leading to the frequent use of untreated natural water sources (Peter-Varbanets et al., 2009). In this scenario, decentralised water treatments offer promising solutions to enhance access to treated water, particularly in remote and rural areas (Xin et al., 2021).

Electro-bioremediation is an innovative technology with notable potential as a decentralised and environmentally friendly water treatment (Pous et al., 2018; Wang et al., 2020). This treatment method relies on primary microbial electrochemical technologies (MET or bioelectrochemical systems, BES) (Schröder et al., 2015). METs utilise the capabilities of electroactive microorganisms to perform selective oxidation and reduction reactions using solid electron conductors (electrodes). In the case of bioelectrochemical nitrate reduction, autotrophic denitrification is accomplished solely using the cathode as an electron donor and inorganic carbon as the carbon source (Puig et al., 2012; Wrighton et al., 2010). Denitrification involves four successive reduction steps, starting with nitrate ($NO_3^-$) and leading to nitrite ($NO_2^-$), nitric oxide (NO), nitrous oxide ($N_2O$) and finally dinitrogen gas ($N_2$). Four reductase enzymes facilitate this process, each responsible for the reduction of a specific intermediate, requiring a total of 5 mol of electrons per mol of nitrate reduced to dinitrogen gas (Vilar-Sanz et al.,

* Corresponding author.
*E-mail address:* sebastia.puig@udg.edu (S. Puig).

https://doi.org/10.1016/j.watres.2024.121618
Received 10 December 2023; Received in revised form 26 March 2024; Accepted 14 April 2024
Available online 15 April 2024

2018; Zhong et al., 2021). Electro-bioremediation offers a significant advantage over other methodologies for nitrate removal by eliminating the need for chemical dosing (e.g., acetate or hydrogen) (Rezvani et al., 2019; Zhao et al., 2022). Instead, the microorganism utilises a solid electrode for the complete conversion of nitrate ($NO_3^-$) into dinitrogen gas ($N_2$) without generating any residue. Consequently, this approach has proven to be more environmentally sustainable than conventional physicochemical methods such as ion-exchange resins and membrane separation, avoiding nitrate-concentrated brine generation and constant chemical consumption. It also exhibits a competitive energy consumption of approximately 0.15 kWh $m^{-3}$ (Pous et al., 2017), in contrast to conventional treatments such as reverse osmosis, nanofiltration and electrodialysis, which consume between 0.54 and 2.06 kWh $m^{-3}$ (Costa and de Pinho, 2006; Twomey et al., 2010).

Currently, electro-bioremediation has undergone validation for the treatment of nitrate-contaminated groundwater on the laboratory-scale (Technology Readiness Level, TRL 3–4). The technology has exhibited promising nitrate removal rates, with a maximum reported rate of 3.7 kg $NO_3^-$ $m^{-3}$ $d^{-1}$, achieved with a cathodic hydraulic retention time ($HRT_{cat}$) of 0.5 h (Pous et al., 2017). Thus, there is an urgent need to scale-up this technology and validate its application in a real-world setting (TLR 5–6). Scaling-up poses a critical challenge for METs, creating a gap between the expectations set by laboratory-scale experiments and the results obtained at pilot-scale. Few attempts in the literature have addressed the challenge of scaling-up METs. Until 2022, only 1 % of the studies in this field focused on the scale-up of this technology (Jadhav et al., 2022). For example, pilot-scale experiments have included the integration of an electrolyser into the anoxic chamber (22 L) of a wastewater treatment plant, resulting in an improvement in nitrogen removal of up to 45 % (Hao et al., 2016). In the field of groundwater treatment, a pilot reactor with a cathodic volume of 4.5 L was tested, although it showed lower nitrate removal rates (below 0.1 kg $NO_3^-$ $m^{-3}$ $d^{-1}$) compared to laboratory results (Lust et al., 2020). Factors such as anode-cathode spacing, redox potential distribution over the electrodes, hydraulics, and mass transfer from liquid to the electrode surface significantly affect the performance of the bioelectrochemical reactors, leading to a decrease in reactor's performance when the size of the reactor is increased (Kadier et al., 2020; Rossi and Logan, 2022). Consequently, the use of reactor volume as the sole scalable factor, a common approach in biological water treatment technologies, is proving ineffective. Thus, compact modular units have been proposed as alternatives for scaling-up METs, allowing for easy connection in series or parallel to form stacked systems (Baeza et al., 2017; Dekker et al., 2009; Flimban et al., 2019).

This study details the design of an *on-site* electro-bioremediation pilot plant, addressing the key challenges of scaling-up a bioelectrochemical system and the real-world constraints of operating in a real-world environment. The research presents the course of *on-site* electro-bioremediation pilot plant for treating nitrate-contaminated groundwater, from start-up to a stable operation, aiming to validate the technology in a relevant environment. The pilot plant was located in Navata, a rural area of Catalonia (Spain), where it consistently treated real nitrate-contaminated groundwater for up to 3 months. The assessment of the electro-bioremediation performance was based on its capacity to reduce nitrate levels without nitrite accumulation. Furthermore, energy consumption was assessed, along with a preliminary cost estimation. Finally, at the end of the experimental study, the reactor was autopsied to analyse the microbial community at different reactor layers to understand the key players in the denitrification process and to identify potential gradients. This study validates electro-bioremediation in a real-world scenario and marks a crucial milestone towards the future implementation of electro-bioremediation as a practical water treatment solution.

## 2. Materials and methods

### 2.1. Bioelectrochemical reactor set-up

A compact tubular bioelectrochemical fixed-bed reactor was built using a polyvinyl chloride tubular structure (PVC, 6.0 cm diameter and 1.7 m length) (Fig. 1). The cathode (inner part) and anode (outer part) compartments were separated with a tubular cation-exchange membrane (diameter 4.5 cm, Catex membranes Ralex®, MEGA, Czech Republic) (Fig. 1). Both compartments were filled with granular graphite as electrode material (average diameter of 3.25 mm, enViro-cell, Germany) with a bed porosity of 50 %, resulting in a net cathode compartment volume (NCC) of 1.2 L and a net anode compartment volume (NAC) of 0.9 L. The estimated cathode surface was 2.2 $m^2$, and the anode surface was 1.7 $m^2$, assuming the granular graphite were perfect spheres with an average diameter of 3.25 mm. Perforated discs (PVC, diameter holds 2 mm) were placed at 25 cm intervals along the cathode compartment to ensure water flow distribution and prevent the granular graphite compaction over the operational study. A titanium rod (6 × 2100 mm, Ti Gr1 ASTM B348, Special metals and products, Spain) was used in the cathode, and a titanium mixed metal oxide rod (Ti-MMO, Special metals and products, Spain) in the anode, serving as cathode and anode current collectors, respectively. A titanium cylindrical mesh (45 × 2000 mm, Ti Gr2 ASTM B265, Special metals and products, Spain) was also installed in the cathode compartment to ensure the correct current and potential distribution along the column. The reactors were equipped with an Ag/AgCl sat. KCl reference electrode (+0.197 V vs. standard hydrogen electrode, SHE, SE 11, Xylem Analytics Germany Sales GmbH & Co. KG Sensortechnik Meinsberg, Germany). Unless otherwise stated, all redox potentials are referred to Ag/AgCl sat. KCl. The reactor was electrically operated by fixing the cell voltage using a power supply while keeping the cathode potential in a range from -0.23 ± 0.03 to -0.67 ± 0.03 V.

The cathode and the anode were hydraulically connected (Fig. 1B). The influent was pumped directly upwards through the cathode compartment, and then it overflowed at the top, entering the anode compartment. It circulated from the top to the bottom of the anode compartment, where a recirculation tank (1.0 L) was positioned before the water was discharged out of the system. The influent flow rates varied from 2.9 to 14.3 L $d^{-1}$ based on the $HRT_{cat}$ tested, with a range from 10.0 to 2.0 h. A portion of the anodic effluent was recirculated to the influent using a second pump at a flow rate of either 100 or 150 L $d^{-1}$, depending on the operational period.

### 2.2. Pilot plant facilities and groundwater characteristics

A container housing the bioelectrochemical reactor and other equipment was installed in Navata (Fig. 1), a rural area in Spain with a population of 1465 inhabitants (2022). This location is characterised by strong livestock and agricultural activities, which have resulted in nitrate contamination of certain aquifers. Specifically, the treated groundwater in this study had an average nitrate concentration of 92.0 ± 7.2 mg $NO_3^-$ $L^{-1}$.

The pilot plant comprised two 1 $m^3$ tanks to store the water extracted directly from a contaminated well. A third tank was used to store the water after undergoing softening treatment (Table 1), which was then treated in the bioelectrochemical reactor. For that purpose, an ion-exchange resin softener (Concept earth line +100, Concept, Spain) was installed and used to reduce the water hardness from 300 to 45 ± 25 mg $CaCO_3$ $L^{-1}$. The resin was periodically regenerated using a NaCl-saturated solution. The groundwater had an oxygen concentration of around 0.5 mg $O_2$ $L^{-1}$ after water extraction and pre-treatment. The container was equipped with an air conditioner to mitigate temperature fluctuations, resulting in a stable temperature of 30 ± 5 °C.

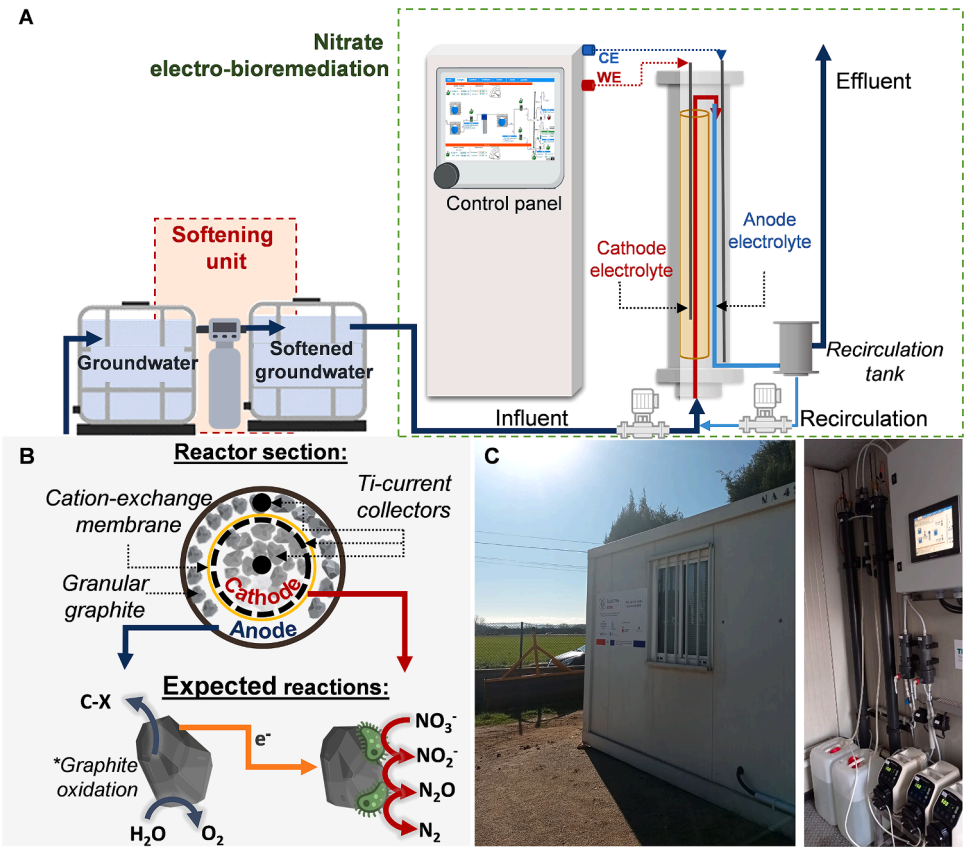


**Fig. 1.** (A) Process outline and diagram of the reactor. (B) Drawing of the reactor section and main reactions expected to occur at anode and cathode. (C) Images of the pilot plant located in Navata (Spain) (left) and the bioelectrochemical reactor (right).

**Table 1**
Groundwater characteristics after pre-treatment by a softening unit during the pilot plant operation, before its treatment in the bioelectrochemical reactor.

| Softened groundwater characteristics | |
|---|---|
| pH | 8.3 ± 0.4 |
| Electrical conductivity (mS $cm^{-1}$) | 0.8 ± 0.1 |
| Water hardness (mS $cm^{-1}$) | 45 ± 25 |
| $NO_3^-$ (mg $L^{-1}$) | 92.0 ± 7.2 |
| $NO_2^-$ (mg $L^{-1}$) | 0.2 ± 0.4 |
| $NH_4^+$ (mg $L^{-1}$) | 0.2 ± 0.3 |
| $Cl^-$ (mg $L^{-1}$) | 56.7 ± 40.6 |
| $SO_4^{2-}$ (mg $L^{-1}$) | 35.5 ± 4.0 |
| $PO_4^{3-}$ (mg $L^{-1}$) | 1.4 ± 6.7 |
| $Na^+$ (mg $L^{-1}$) | 144.9 ± 47.3 |
| $Mg^{2+}$ (mg $L^{-1}$) | 2.6 ± 2.4 |
| $Ca^{2+}$ (mg $L^{-1}$) | 29.0 ± 27.2 |
| $K^+$ (mg $L^{-1}$) | 4.2 ± 4.0 |

### 2.3. Inoculation protocol

The bioelectrochemical reactor was inoculated in a batch flow mode, applying a recirculation of 100 L $d^{-1}$ to promote a proper flow distribution and homogeneity in the reactor. The reactor was filled with 50 % synthetic groundwater and 50 % inoculum. The inoculum consisted on the effluent of a previous running reactor (Ceballos-Escalera et al., 2021), which was stored under $H_2$:$CO_2$ (80:20 %) atmosphere and periodically supplemented with nitrate to a theoretical concentration of 145.0 mg $NO_3^-$ $L^{-1}$. The synthetic groundwater mimicked the characteristics of Navata's groundwater but was amended with all requirements for the denitrifying bacteria to grow (e.g., trace elements). Synthetic medium contained (per L): 0.42 g $NaHCO_3$, 0.20 g $NaNO_3$ (145.0 mg $NO_3^-$ $L^{-1}$), 0.08 g $KH_2PO_4$, 0.02 g $Na_2HPO_4$, 0.1 g NaCl, 0.75 g $MgSO_4 \times 7H_2O$, 0.01 g $NH_4Cl$ and 0.1 mL of trace element solution (Balch et al., 1979).

During the batch inoculation period, the cell voltage was fixed at 1.08 ± 0.14 V, resulting in a cathode potential of −0.38 ± 0.19 V vs. Ag/AgCl, which was expected to promote denitrification (Pous et al., 2015). After 4 days of the batch process, the nitrate concentration decreased from 110.7 to 5.5 mg $NO_3^-$ $L^{-1}$, and a concentrated nitrate solution was added to increase again the nitrate concentration to 359.0 mg $NO_3^-L^{-1}$. The inoculation process lasted 11 days when stable current density (12.5 A $m^{-3}_{NCC}$) was achieved.

### 2.4. Continuous flow mode operation

The reactor operated continuously for 3 months, with a focus on evaluating its performance under varying cathodic hydraulic retention times ($HRT_{cat}$). Following the inoculation of the reactor in batch mode, real nitrate-contaminated groundwater was treated in continuous flow mode at an $HRT_{cat}$ of 10 h. Throughout this period, the $HRT_{cat}$ was progressively reduced to 2.0 h. The reduction was 20 % between $HRT_{cat}$ of 10.0 h and 5.1 h, and subsequently, each reduction was 35 % until $HRT_{cat}$ of 2.0 h. Each step of $HRT_{cat}$ was tested for a minimum of 7 days and included at least 3 sample replicates. From day 0 to day 60, the $HRT_{cat}$ was reduced from 10.0 to 2.0 h, and the recirculation flow rate was set at 100 L $d^{-1}$. From day 60 to 90, the $HRT_{cat}$ was kept constant at 2.0 h, and the recirculation rate was increased to 150 L $d^{-1}$. The cell voltage was gradually increased from 1.22 ± 0.02 to 1.72 ± 0.05 V to keep the cathode potential within the specified range of -0.23 ± 0.03 to -0.67 ± 0.03 V (Ceballos-Escalera et al., 2021).

### 2.5. Analytical methods for liquid samples

Samples were taken and analysed 2–3 times per week, resulting in a

minimum of three analytical measurements for each condition. All liquid samples were analysed in the laboratory by ionic chromatography (ICS 5000, Dionex, USA) according to APHA standard water measurements (APHA, 2005) with special attention to these ions: nitrate ($NO_3^-$), nitrite ($NO_2^-$), and ammonium ($NH_4^+$). The pH and electrical conductivity of the samples were measured using a pH-meter (pH-meter basic 20+, Crison, Spain) and a conductivity-meter (EC-meter basic 30+, Crison, Spain), respectively. Nitrous oxide ($N_2O$) was measured *in-situ* over the last $HRT_{cat}$ of 2.0 h using an $N_2O$ liquid-phase microsensor (Unisense, Denmark) located in the recirculation loop of the reactor. The softened groundwater hardness was periodically examined (Total Hardness Test Method, titrimetric with titration pipette MQuant®, Merck, USA).

### 2.6. Microbial community structure analysis

At the end of the experimental study, the reactor was autopsied in terms of microbial community. The cathode compartment was segmented into seven different layers along its length (sections of 25 cm long). Granular graphite samples were collected to analyse the microbial community of each section, where a single sample was collected from each section by mixing the granular graphite from the specific section ($n = 1$). Samples from the initial inoculum ($n = 3$) and the reactor effluent ($n = 1$, day 75) were also analysed.

The microbial community structure and taxonomical classification of relevant bacteria in the studied bioreactor were determined using barcoded amplicon-based Illumina sequencing of the partial 16S rRNA gene. For liquid samples (inocula and effluent), cells were recovered after centrifugation of 4 to 10 mL (4500 rpm, 10 min, 4 °C). For the biofilm, 0.5 g of crushed electrode material was used directly for extraction. In both cases, DNA was extracted using the FastDNA® SPIN Kit for soil (MP, Biomedicals, Santa Ana, California, EUA), according to the manufacturer's instructions. The obtained DNA was quantified using a NanoDrop ND-1000 spectrophotometer (Nano. Drop Technologies, Inc., Wilmington, DE) and stored at −20 °C. Illumina MiSeq flow cell (V2) sequencing was conducted by the RTSF Core facilities at the Michigan State University USA (https://rtsf.atsci.msu.edu/). The primers set 515F and 806R were used for the amplification of the V4 region of 16S rDNA (Kozich et al., 2013). Raw sequencing data were quality filtered, trimmed, dereplicated, merged, and after chimera removal, were clustered into amplicon sequence variants (ASVs) using the DADA2 Pipeline (Callahan et al., 2016).

Taxonomic assignations were done using the Silva 138.1 database as a reference (www.arb-silva.de). ASVs not assigned at the phylum level, as well as those assigned to Mitochondria or Chloroplast, were removed from the Taxa table. Singletons, if arising during data processing, were also removed from the data set. When needed, taxonomic assignations were refined by BLASTn searches using the refseq_rna database as a reference and excluding environmental isolates (blast.ncbi.nlm.nih.gov). The final number of ASVs in the data set was 1971. From these, 297 (15.1 %) could not be assigned to the Family level. Average number of reads per sample was 39,816, ranging from 27,121 to 61,724. Rarefaction to an even sequencing depth was not applied. The relative abundance of ASVs was calculated as per sample basis using the phyloseq package in R. The potential for denitrification (either complete or partial) and ammonification of found ASVs was inferred from KEGG functional annotations of genomes of the closest relative to the obtained sequence. The raw data files containing sequences analysed in this work have been deposited in the Sequence Read Archive (SRA-NCBI) under Bioproject accession number PRJNA1042638.

### 2.7. Calculations: nitrate removal rate, energy consumption and cost estimation

The hydraulic retention time was calculated considering the NCC ($HRT_{cat}$), as denitrification takes place in this compartment. Nitrate reduction rates were determined by measuring the concentration difference between influent and effluent, normalised by the NCC (kg $NO_3^-$ $m^{-3}$ $d^{-1}$) (Eq. S1, Supplementary data). Energy consumption to support bio-/electrochemical reactions was calculated by multiplying the observed cell voltage and current (Eq. S5, Supplementary data) and expressed relative to the amount of nitrate removed (kWh $kg^{-1}$ $NO_3^-$) or the volume of water treated (kWh $m^{-3}$). The coulombic efficiency of the denitrifying biocathode ($CE_{cat}$) was determined according to (Pous et al., 2017), dividing the actual measured current in the system by the calculated theoretical current, which accounted for incomplete reduction up to nitrite (Eq. S4-S6 in Supplementary data).

Capital, Operational and Total expenditures (CAPEX, OPEX and TOTEX, respectively) were estimated for a single module. Detailed information can be found in Table S1 of the Supplementary Data. The CAPEX was determined based on the actual cost of the materials used for assembling the reactor. The cost of the pumps was adjusted to reflect more realistic scenarios, replacing peristaltic pumps with centrifugal pumps. The OPEX was estimated based on the energy consumption of the recirculation pump according to its technical specifications and the power supply connected to the bioelectrochemical reactor (as described in Eq. S5 in the Supplementary Data). The electricity price for industrial consumers from the second period of 2022 in Europe was used in the calculation (Eurostat statistics, 0.20 € $kWh^{-1}$). The OPEX estimation also included maintenance costs, accounting for 3 % of the CAPEX (Jourdin et al., 2020). Both CAPEX and OPEX costs were normalised based on the treatment capacity of each module ($m^{-3}$) and assuming a module lifespan and amortisation period of 30 years. TOTEX was calculated as the sum of OPEX and CAPEX.

## 3. Results and discussion

### 3.1. Electro-bioremediation validation at the on-site pilot plant: removal rate, energy consumption, and effluent quality

The *on-site* electro-bioremediation pilot plant was operated continuously over three months (Fig. 2), following an initial fast start-up period of 11 days in batch mode. During the first 24 days under continuous flow mode, the reactor was operated at an $HRT_{cat}$ of 10 h. At the end of this period, a nitrate removal efficiency of 99 % was achieved.

Subsequently, the $HRT_{cat}$ was gradually decreased from 10.0 to 2.0 h. During this period, the cell voltage was linearly increased from 1.22 ± 0.02 to 1.58 ± 0.05 V in response to the increasing nitrate loading rate (Fig. S2, Supplementary data) and, consequently, the expected current density (Ceballos-Escalera et al., 2021; Pous et al., 2017). This was done to keep the cathode potential within a range suitable for bioelectrochemical denitrification (-0.23 ± 0.03 to -0.62 ± 0.09 V) (Pous et al., 2015) but preventing uncontrolled hydrogen ($H_2$) evolution (cathode potentials below -0.70 V) (Batlle-Vilanova et al., 2014). During the transition from 10.0 to 3.1 h $HRT_{cat}$, the nitrate removal efficiency remained largely stable at 97 ± 5 %. As a result, the nitrate removal rate increased from 0.2 ± 0.0 to 0.6 ± 0.1 kg $NO_3^-$ $m^{-3}$ $d^{-1}$. Despite a further reduction of $HRT_{cat}$ to 2.0 h and an increase of the cell voltage to 1.58 ± 0.05 V, there was no further increase in the nitrate reduction rate. It remained stagnant at 0.7 ± 0.0 kg $NO_3^-$ $m^{-3}$ $d^{-1}$, with no significant difference from the previous $HRT_{cat}$ of 3.1 h (*t*-tests, *p-value* 0.17). As a result, the nitrate removal efficiency decreased to 65 ± 3 %. Following previous research demonstrating the importance of recirculation flow rates to ensure optimal nitrate removal performance (Ceballos-Escalera et al., 2021), the recirculation rate was increased from 100 to 150 L $d^{-1}$ on day 68. Simultaneously, the cell voltage was raised from 1.58 ± 0.05 V to 1.72 ± 0.05 V (decreasing the cathodic potential to -0.67 ± 0.03 V). This setting proved to be effective as the nitrate removal rate increased significantly to 0.9 ± 0.1 kg $NO_3^-$ $m^{-3}$ $d^{-1}$, corresponding to a nitrate removal efficiency of 82 ± 18 %.

The nitrate removal rate results are consistent with the typical range reported for laboratory-scale bioelectrochemical reactors operating in continuous flow mode, which is in the range of 0.1 to 1.0 kg $NO_3^-$ $m^{-3}$ $d^{-1}$

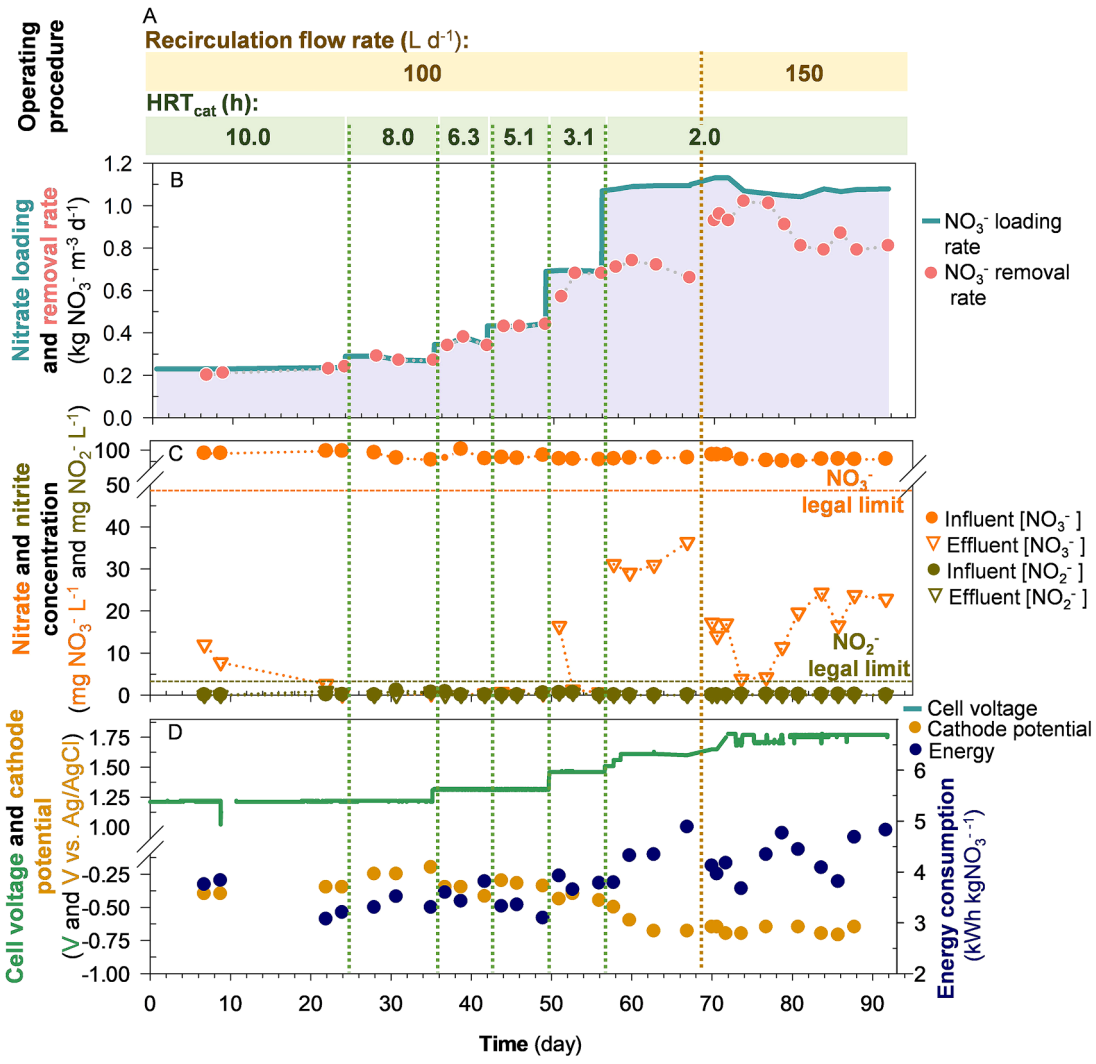


**Fig. 2.** Overview of the key operating parameters over the three months of operation. (A) Operational procedure in terms of recirculation rate and $HRT_{cat}$. (B) Nitrate loading and removal rate. (C) The nitrate and nitrite concentrations in the influent and effluent are represented with circles and triangles, respectively; the guideline values according to the European Directive 2020/2184 are represented with a solid line. (D) Fixed cell voltage and the resulting cathode potential, current density and energy consumption.

(Gadegaonkar et al., 2023). For example, in a similar set-up for groundwater treatment, Cecconet et al. (Cecconet et al., 2018) reported a nitrate reduction rate of 0.3 kg $NO_3^-$ $m^{-3}$ $d^{-1}$ with a high efficiency of 94 % at an $HRT_{cat}$ of 15.6 h. A few laboratory studies have reported higher rates up to 3.7 kg $NO_3^-$ $m^{-3}$ $d^{-1}$ at an $HRT_{cat}$ of 0.5 h (Pous et al., 2017). However, this study showed a low nitrate reduction efficiency (50 %), resulting in an effluent nitrate concentration of 72 mg $NO_3^-$ $L^{-1}$, which exceeds the guideline limit of the European Directive. In contrast, the laboratory-scale study used to design this pilot plant showed a nitrate reduction rate of 2.3 kg $NO_3^-$ $m^{-3}$ $d^{-1}$ at $HRT_{cat}$ of 1.5 h, achieving a nitrate reduction efficiency of 90 % (Ceballos-Escalera et al., 2021). However, as the scale increased, the rates decreased drastically. Lust et al. (Lust et al., 2020) showed a pilot-scale reactor in batch mode with nitrate reduction rates below 0.1 kg $NO_3^-$ $m^{-3}$ $d^{-1}$. The achieved nitrate reduction rate of 0.9 kg $NO_3^-$ $m^{-3}$ $d^{-1}$ in the pilot plant presented in this study, with a nitrate removal efficiency of 82 ± 18 % at $HRT_{cat}$ of 2.0 h, highlights am optimistic technology transition to the operation of an *on-site* electro-bioremediation pilot plant. This represents an important step in bridging the gap between laboratory expectations and pilot-scale results, although there is still room for operational improvement to achieve higher nitrate reduction rates at the pilot plant compared to results obtained on a smaller scale under controlled laboratory conditions. Certain factors may have directly influenced this lower treatment capacity, requiring operation at higher $HRT_{cat}$ and, consequently, a lower nitrate reduction rate. These factors include the larger scale and water characteristics. For example, although the design used in this reactor attempts to address the heterogeneous distribution of redox potential along the reactor by installing current collectors, it could still affect performance. Therefore, this aspect needs to be further considered in future reactor designs. Treatment of real groundwater also affects performance. The lower nitrate concentration in the treated groundwater (92 ± 5 mg $NO_3^-$ $L^{-1}$) compared to other laboratory-scale studies (169 ± 5 mg $NO_3^-$ $L^{-1}$, (Ceballos-Escalera et al., 2021)) led to different nitrate removal rates for similar $HRT_{cat}$. In addition, factors within the water matrix, such as the lower electrical conductivity of real groundwater (<0.8 mS $cm^{-1}$), could potentially limit denitrification (Puig et al., 2012). Furthermore, the absence of certain trace elements (e.g. Fe, Mn and Zn) in real groundwater that are present in synthetic groundwater may affect the denitrification process (Labbé et al., 2003). Therefore, future tests in different environments are crucial to fully explore the potential of nitrate electro-bioremediation.

The system demonstrated remarkable efficiency in converting nitrate to dinitrogen gas, with a mean coulombic efficiency of 113 ± 9 % at the last $HRT_{cat}$ of 2.0 h. Such denitrification can be supported by the use of

the cathode as an electron donor and/or by the use of hydrogen produced as a cathodic reaction. However, it has previously been shown that this hydrogen production is marginal at potentials higher than -0.70 V in granular graphite cathodes (Batlle-Vilanova et al., 2014). Therefore, a small contribution of hydrogen-mediated denitrification is expected in the studied reactor, where the cathode potential ranged between -0.23 ± 0.03 and -0.67 ± 0.03 V. CEs higher than 100 % can be explained by the complexity of real groundwater, which may contain unidentified electron donors (e.g., organic matter, iron or sulphur) that might be used as electron donors for denitrification (Rivett et al., 2008). Additionally, this could be attributed to the potential accumulation of intermediate denitrification (e.g., nitrous oxide, as will be discussed later) since CE calculations only considered nitrite accumulation. Even so, the CEs observed in this work (113 ± 9 %, at 2.0 h $HRT_{cat}$) indicate effective and selective nitrate removal, minimising energy losses associated with oxygen reduction or other compound reduction such as sulphate. Besides, this supports that no uncontrolled/unused $H_2$ was produced by the system. Consequently, the energy consumption attributed to electrochemical reactions remained mostly stable throughout the operational study (0.32 ± 0.03 kWh $m^{-3}$). In terms of specific energy consumption normalised to nitrate removal, the energy consumption fluctuated between 3.5 ± 0.4 and 4.3 ± 0.4 kWh $kg^{-1}$ $NO_3^-$ at an $HRT_{cat}$ of 10.0 and 2.0 h, respectively (Fig. 2C).

Ensuring high-quality effluent is crucial to validate electro-bioremediation as a water treatment method. Over three months of continuous operation (Fig. 2B), the effluent consistently met drinking water standards for nitrate compounds (<50.0 mg $NO_3^-$ $L^{-1}$, European Directive 2020/2184 ). The nitrate concentration ranged from 0.1 ± 0.2 mg $NO_3^-$ $L^{-1}$ at an $HRT_{cat}$ of 8.0 h to 15.9 ± 7.1 mg $NO_3^-$ $L^{-1}$ at the final $HRT_{cat}$ condition of 2.0 h (with a recirculation rate of 150 L $d^{-1}$), which showed the highest nitrate reduction rate. In optimal biological denitrification, nitrate is converted to dinitrogen gas. However, in some situations, denitrification can get stuck at undesired intermediates, such as nitrite or nitrous oxide. Dissimilatory denitrification could also occur, leading to the conversion of nitrate to ammonium. (European Directive 2020/2184 sets limits for the presence of nitrite and ammonium in drinking water at 0.5 mg $NO_2^-$ $L^{-1}$ and 0.5 mg $NH_4^+L^{-1}$, respectively. The levels of nitrite and ammonium in the effluent of the electro-bioremediation reactor consistently met these guidelines (0.1 ± 0.3 mg $NO_2^-L^{-1}$ and 0.1 ± 0.1 mg $NH_4^+$ $L^{-1}$). The lowest $HRT_{cat}$ of 2.0 h, which exhibited the best performance in terms of nitrate reduction rate, was further investigated for the presence of nitrous oxide. Specifically, the dissolved nitrous oxide concentration at this condition was 15.2 ± 2.1 mg $N_2O$ $L^{-1}$, corresponding to 26 ± 4 % of the nitrate removed during that specific period (Fig. S1, Supplementary data). Although nitrous oxide is not subject to regulation, its mitigation holds significant importance due to its contribution to the greenhouse effect. The low $HRT_{cat}$ of the system, an inappropriate cathode potential or even the microbial community (discussed later) may be responsible for their occurrence (Pous et al., 2015; Zhao et al., 2022).

Considering all these factors, the electro-bioremediation system demonstrated its suitability as a water treatment approach for achieving the required effluent quality in the tested site. However, further research is required at additional contaminated sites to fully validate electro-

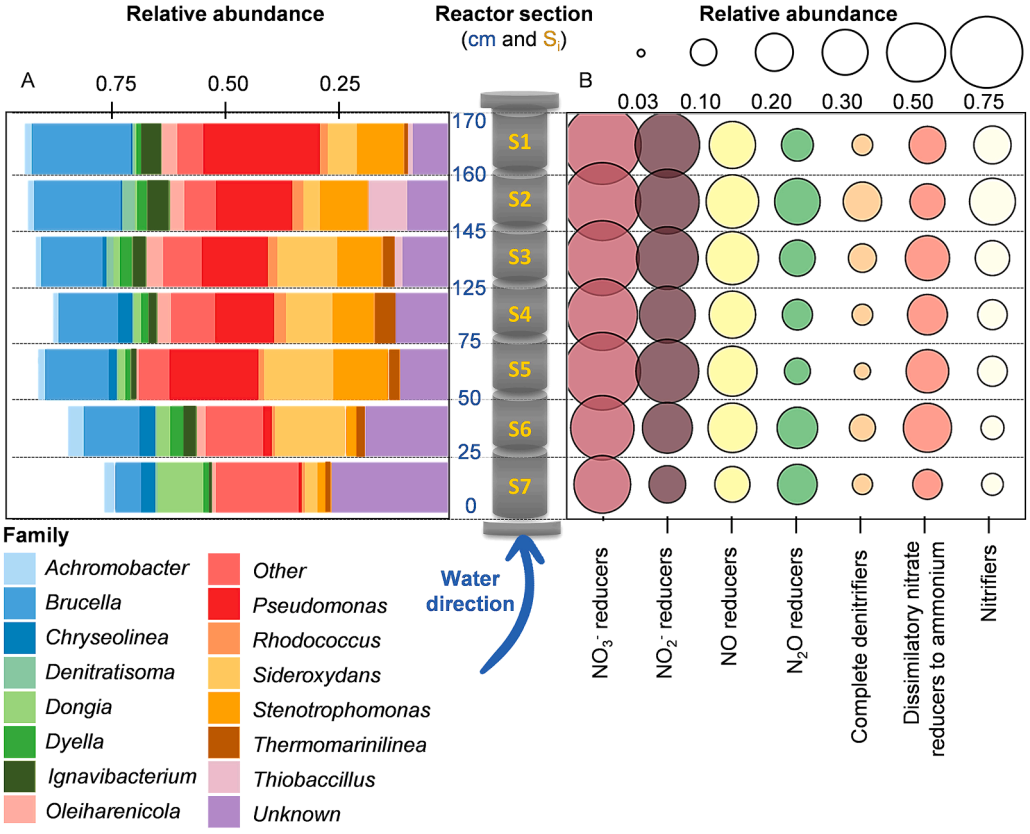


**Fig. 3.** An overview of microbial community stratification in the biocathode is presented. The reactor is divided into sections ($S_i$), and their respective positions in cm (centre of the figure) are indicated with respect to the inflow direction from bottom to top. (A) Stacked bar plot of relative abundances of the most abundant ASV per sample, including their taxonomical assignation at the Genus level. Other- genera that were found at less than 0.5 % or in a single sample. Unknown- Sequences that could not be classified to Genus level. (B) Relative abundance (according to the total number of 16S rRNA reads per sample) of microorganisms with potential activities related to the Nitrogen cycle. Functional groups were predicted according to the presence of key relevant genes in the genome of the closest relative to the obtained sequence. $NO_3^-$ reducers, presence of napA or narG genes; $NO_2^-$ reducers, presence of nirS or nirK genes, NO reducers, norB genes; $N_2O$ reducers, nosZ genes; dissimilatory nitrate reducers to ammonium, nrfA or nirB genes; Nitrifiers, amoA genes. Complete denitrifiers were defined as those genomes harbouring narG or napA, nirS or nirK, norB and nosZ genes.

bioremediation. This will include testing higher nitrate concentrations, although laboratory-scale results indicate that there is no limitation to achieving desired nitrate reduction efficiencies and effluent quality at higher nitrate loading rates (Ceballos-Escalera et al., 2021).

## 4. Microbial dissection of the biocathode: revealing the key players in denitrification

The microbiological composition formed as a biofilm on the granular graphite of the different sections of the reactor was analysed at the end of the experimental period (Fig. 3). The microbiome presented significant differences from previous laboratory-scale reactors used as inoculum (Ceballos-Escalera et al., 2021). An ordination analysis of samples based on distance similarities of microbial community compositions showed a clear separation between inoculum and reactor samples (Fig. S3, Supplementary data). At the family level, members of *Acidithiobacillaceae, Comamonadaceae* and *Rhodocyclaceae*, which were abundant in the inoculum (data extracted from (Ceballos-Escalera et al., 2021)), were replaced by *Pseudomonadaceae, Rhizobiaceae, Gallionellaceae* and *Xanthomonadaceae* as the most abundant groups in the biocathode.

To gain insight into the biocathode and to detect spatial differences in the microbial community composition, the 90 most abundant ASVs were selected per sample basis and analysed. On average, this sub-set of highly represented microorganisms accounted for 86 % of total reads in graphite samples (from 70to 90 %, depending on the considered sample, Fig. 3A), thus constituting a highly representative fraction of the microbial community. The composition of microbial communities developing as biofilms in the tubular reactor yielded some heterogeneities along the longitudinal axis (Fig. 3A). At the community level, diversity indices were higher in the lower sections of the reactor (sections S6 and S7, from 5 to 50 cm) compared to the upper part. For instance, richness, the number of different ASVs, decreased from 547 (S7) to 307 (S1), probably indicating a specialisation of microbial communities to the conditions applied to the column, being less affected by the incoming groundwater (S7). The presence of oxygen from incoming groundwater could have potentially limited the development of a robust and stable denitrifying community at lower sections. For instance, in section S7, the most abundant microorganism was *Dongia*, an aerobic bacterium whose denitrification capacity has not been proven (Kim et al., 2016). After the first 25 cm of the reactor, the relative abundance of *Sideroxydans*-related sequences significantly increased and remained at higher levels in the central part of the reactor (S6 to S3), which is characterised by denitrification capacity (He et al., 2016). In contrast, the microbial community appeared to be progressively enriched in *Pseudomonas, Brucella*, and *Stenotrophomonas*-related species in sections S1 to S5. All groups enriched in these areas are characterised to contain members with a proven denitrification capacity (Ghosh et al., 2020; Solera and Castaño, 2008; Zhang et al., 2021).

Further analysis of potential functions in each reactor section, specifically related to the nitrogen cycle, was performed after predicting functional groups from taxonomic data. The presence of genes in annotated genomes that showed high similarity (>95 %) to the obtained partial 16S rRNA sequences were used to classify functional groups (see Fig. 3 caption). Potential nitrate and nitrite reduction capacity remained high throughout the reactor and was relatively higher to all other defined groups (Fig. 3B). The estimated relative abundance of nitrate and nitrite reducers was higher in the upper part (S1 to S4). The incoming groundwater contained a higher oxygen concentration, potentially inhibiting the nitrate and nitrite reduction which would agree with the lower relative abundance of nitrate and nitrate reducers in sections S6 and S7. Numerous nitrate and nitrite reducers are facultative bacteria capable of aerobic growth (Lycus et al., 2017) thus high relative abundances of NAR (60.5 ± 13.2 %) and/or NIR (38.7 ± 12.4 %) harbouring bacteria trough the reactor column were not unexpected. Putative nitrogen monoxide reductases (NOR) containing bacteria showed a similar trend, with a lower relative abundance at the water inlet section (S6 and S7) whereas the occurrence of bacteria carrying genes related to nitrous oxide reduction (NOS-related genes) was lower. This observation would suggest the formation of nitrous oxide gas within the system, although additional analyses (i.e. enzyme activity measurements) would be needed to confirm this hypothesis. Genetic potential for nitrous oxide accumulation due to changes in the abundance of NIR/NOS ratio in natural environments or bioelectrochemical reactors has been previously confirmed using quantitative PCR of selected genes (García-Lledó et al., 2011; Vilar-Sanz et al., 2013). Alternatively, organisms potentially harbouring a complete gene set for denitrification accounted for less than 10 % in all samples except in section S2 (17 %). This finding reinforces the concept that, in the conditions employed, complete denitrification was a cooperative process. Finally, the predicted presence of microorganisms carrying *nrf*A genes suggests a potential for putative dissimilatory nitrate reduction to ammonium, more pronounced in sections S3 to S6. Nevertheless, ammonium accumulation within the treated water remained marginal (0.1 ± 0.1 mg $NH_4^+$ $L^{-1}$). Conversely, the capacity for ammonium oxidation was more prominent in sections S1 and S2.

The microbial community analysis highlighted some heterogeneities in terms of composition and the relative abundance of functional groups. This highlights the need for improvements to ensure consistent conditions in order to have a homogeneous reactor with similar capacities in the whole reactor.

## 5. Techno-economic analysis: how to make electro-bioremediation implementation feasible?

The previous sections have demonstrated the feasibility of transitioning electro-bioremediation from the laboratory to the *on-site* pilot plant in terms of nitrate removal and effluent quality. However, estimating the capital (CAPEX) and operational (OPEX) costs is essential to validate its potential for commercialisation and implementation, based on the achievement in the studied pilot plant as well as in some hypothetical scenarios (Fig. 4). Additionally, it is imperative to evaluate the social and environmental benefits of this water treatment technology, as it provides additional value.

The cost estimation in this study specifically targeted a single electro-bioremediation module. The technology would be scaled-up by stacking different modules together. Based on the optimal conditions observed in the pilot plant for nitrate removal rate at an $HRT_{cat}$ of 2.0 h (Fig. 4A, scenario 1), an OPEX of 0.40 € $m^{-3}$ was estimated. The only consumable was electricity with a cost of 0.20 € $m^{-3}$, considering the price for industrial consumers from the second period of 2022 in Europe (Eurostat statistics, 0.20 € $kWh^{-1}$). Electricity was required for the water recirculation pump (0.13 € $m^{-3}$) and the power supply required for the bioelectrochemical reaction (0.06 € $m^{-3}$). It is crucial to consider that electricity costs can vary significantly due to price fluctuations over time (e.g., the period from 2021 to 2022 increased the average price in Europe by 93 %) and location. The employment of renewable energy sources *on-site* would reduce these costs. The estimated OPEX also included reactor maintenance (0.20 € $m^{-3}$), which is calculated as 3 % of the CAPEX. Overall, the OPEX demonstrated competitive costs compared to other treatments. For instance, nanofiltration showed an OPEX ranging from 2.21 to 0.14 € $m^{-3}$ based on treatment flow, considering an electricity price of 0.08 € $kWh^{-1}$ (Alavijeh et al., 2023). Notably, this nanofiltration treatment is characterised by significant environmental impacts, including water rejection and brine generation.

The CAPEX of the single electro-bioremediation module (including the reactor and the recirculation pump) was estimated to be 6.65 € $m^{-3}$ (at $HRT_{cat}$ 2.0 h), assuming a life span of 30 years (Fig. 3A). This brought the TOTEX to 7.05 € $m^{-3}$. This cost is consistent with the water tariffs for households in Europe, which are regulated by the governments or provided by the operators. For instance, the price of water for household use in 2020 ranged from 1.07 € $m^{-3}$ (Bulgaria) to 9.32 € $m^{-3}$ (Denmark)

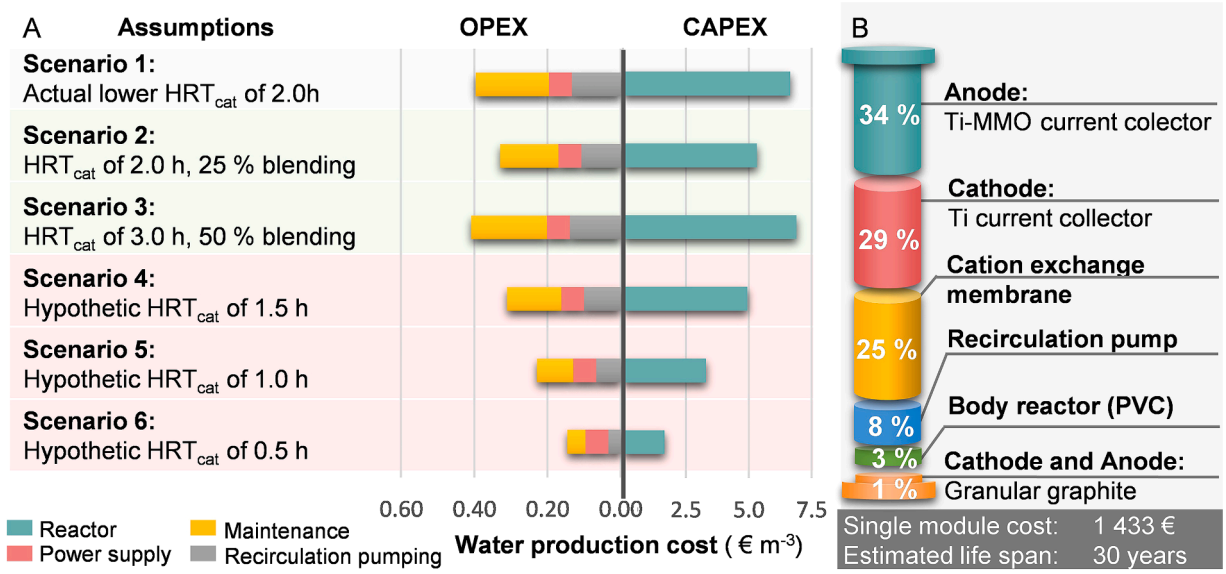


**Fig. 4.** Summary of Capital Expenditure (CAPEX) and Operating Expenditure (OPEX) costs for the electro-bioremediation pilot plant. (A) OPEX and CAPEX are normalised based on the amount of water production across various scenarios. Scenario 1 represents the costs under the conditions where the maximum nitrate reduction rate was observed. Scenarios 2 and 3 involve a blending of a fraction of non-treated groundwater. Scenarios 4–6 are hypothetical scenarios that assume an improvement in the treatment capacity of the system. (B) The total cost of a single module provides a breakdown of the expenses involved.

(EurEau, 2020). However, although the OPEX is competitive (0.4 € $m^{-3}$), the CAPEX is still not (94 % of TOTEX).

Therefore, it appears essential to reduce CAPEX and, consequently, the TOTEX to improve the overall competitiveness of the technology. Two primary approaches have been estimated: (i) increasing water production per module and (ii) reducing the cost of materials used. Given that the treatment significantly reduces nitrate concentrations, the treated water can be blended with untreated water to increase water production while still meeting drinking water standards. However, even under hypothetical conditions of operating at an $HRT_{cat}$ of 2.0 h and blending the effluent with 25 % non-treated water, the TOTEX would remain high (5.65 € $m^{-3}$) (Fig. 3A, scenario 2). Similarly, if operating at an $HRT_{cat}$ of 3.1 h to achieve lower nitrate concentrations at the electro-bioremediation effluent (6.1 ± 8.9 mg $NO_3^-$ $L^{-1}$), which allows for a 50 % blending with untreated water, the TOTEX would increase to 7.31 € $m^{-3}$ (see Fig. 4A, scenario 3). Nevertheless, the economic viability could be significantly improved by hypothetically increasing the water treated per module, ensuring good effluent quality when operating the reactor at $HRT_{cat}$ lower than those reached in this work (Fig. 4A scenarios 4–6). For instance, the TOTEX could be reduced to a more competitive price of 1.80 € $m^{-3}$ by operating the reactor at an $HRT_{cat}$ to 0.5 h, which is close to the shortest reported in the literature at laboratory-scale (Pous et al., 2017).

In terms of the initial investment, each module had a cost of 1433 € (Fig. 4B). The primary cost of the reactors was attributed to the current collectors, representing 63 % of the cost (Fig. 3B). Current collectors were important for scaling-up the reactor in terms of correct redox potential distribution. However, cost reduction of current collectors is crucial for achieving the feasibility and competitiveness of electro-bioremediation. A simpler current collector, for instance, removing the titanium cylindrical mesh in the cathode, may reduce the total cost by 23 %. Additionally, alternative materials could be considered (e.g., stainless steel) or developed to reduce this cost. Nevertheless, it is important to note that the selected material (titanium) provided high stability, ensuring a long lifespan. In parallel, operating the pilot plant with a minimum $HRT_{cat}$ of 2.0 h resulted in a treatment capacity of 14 L $d^{-1}$. In a hypothetical scenario where the aim is to treat 1 $m^3$ $d^{-1}$, 70 modules would be required. This highlights the need to increase the treatment capacity of each module. Theoretically, by improving the $HRT_{cat}$ to 0.5 h (57 L $d^{-1}$ for each module), it could be estimated that only 18 modules would be needed to achieve a daily treatment of 1 $m^3$.

### 5.1. *Factors that influence the successful scaling-up and the subsequent steps for future implementation: comparative analysis between laboratory and pilot plant performance*

The implementation of an *on-site* electro-bioremediation pilot plant entails various influential factors that must be considered. This study addressed not only the challenges associated with reactor scale-up, but also the operational concerns associated with the groundwater matrix and uncontrolled conditions in the on-site operating environment (Fig. 5). Scaling-up bioelectrochemical reactors poses several challenges regarding reactor design. For instance, the distance between the electrodes was selected as a design parameter due to its impact on the performance, as observed in previous attempts (Papillon et al., 2021). To address this, the reactor was scaled-up by keeping the diameter used in the laboratory-scale experiments but increasing the reactor length (Ceballos-Escalera et al., 2021). To prevent the formation of unwanted preferential channels due to the length of the reactor, perforated discs were installed every 25 cm along the reactor. These discs not only redirected the water flow upwards but also prevented the compaction of the granular graphite during operation.

Granular graphite is employed as the electrode material in both the cathode and anode compartments due to its compatibility with microorganism growth and high volume-to-surface ratio. Specifically, in the cathode, granular graphite increases the electrode surface to enhance denitrification. Meanwhile, in the anode, granular graphite can be oxidised, reducing water oxidation as an anodic reaction that can lead to excessive oxygen accumulation in the system (Lai et al., 2017). Nonetheless, the main drawback is its lower electrical conductivity ($10^{-2}$ Ω m). To overcome this, two types of current collector were used in the cathode: a central titanium rod and a surrounding cylindrical titanium mesh. This approach aimed to promote uniform current distribution and reduce redox potential variation, even with a reactor length of 1.7 m (Quejigo et al., 2021). The increase in reactor length also raised concerns about the real effect of a potentiostatic strategy in all parts of the reactor, leading to the adoption of a more flexible electric control strategy. Thus, the cell voltage was controlled to maintain the cathode

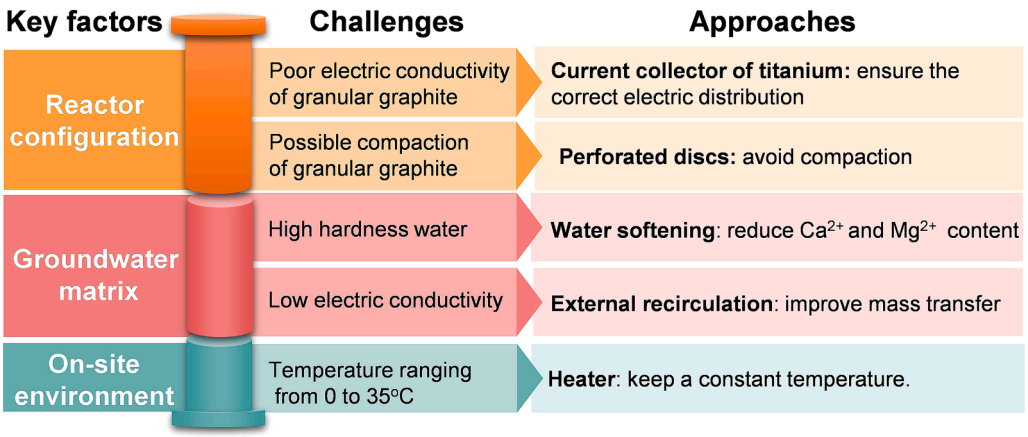


**Fig. 5.** Comprehensive overview of the key factors and associated challenges that require focused attention over the design and operation of a pilot plant in a real environment.

potential in a flexible range between -0.23 ± 0.03 and -0.67 ± 0.03 V throughout different operational periods (Fig. 2). This range was carefully chosen to promote denitrification throughout the reactor, preventing the formation of zones where denitrification is thermodynamically unfavourable (Pous et al., 2015) and minimising uncontrolled hydrogen ($H_2$) production at cathodic potentials lower than -0.70 V (Batlle-Vilanova et al., 2014). The energy consumption in the pilot plant (4.3 ± 0.4 kWh $kg^{-1}$ $NO_3^-$) was even lower than in the laboratory-scale (6.3 ± 0.3 kWh $kg^{-1}$ $NO_3^-$) (Ceballos-Escalera et al., 2022). This emphasises that overcoming the challenge of larger electrodes is feasible with the right considerations. Nevertheless, as mentioned above, addressing current collector costs and maintaining pilot-scale performance requires further investigation.

Additionally, prior groundwater assessment is crucial before implementing electro-bioremediation. The high water hardness (300 mg $CaCO_3$ $L^{-1}$) at the Navata site posed potential scaling problems in the reactor, specifically in the biocathode (Ceballos-Escalera et al., 2022). Thus, a conventional ion-exchange resin softener was implemented to prevent long-term treatment failure, reducing hardness levels to 45 ± 25 mg $CaCO_3$ $L^{-1}$ in this study. At the end of the operational study, the reactor was autopsied, and no signs of scaling were detected (photo shown in Fig. S4, Supplementary data). Other physicochemical parameters, such as pH and electrical conductivity, also play crucial roles. While the influent pH (8.3 ± 0.4) was sustainable for denitrification, the low electrical conductivity of 0.8 ± 0.1 mS $cm^{-1}$ was expected to limit bioelectrochemical denitrification (Puig et al., 2012). When electrical conductivity is low, the transfer of charge-balancing ions, such as protons, can be limited. To address this issue, recirculation has been implemented as an operational strategy to overcome this limitation. Increasing the recirculation rate to enhance denitrification was demonstrated to be an effective strategy, initially in laboratory-scale experiments (Ceballos-Escalera et al., 2021) and subsequently in the pilot plant.

The last aspect considered was the less controlled conditions associated with *on-site* treatment, such as climatic conditions. Navata has a Mediterranean climate, with temperatures ranging from a high of 35 °C during summer to a low of 0 °C in winter. Lower temperatures have a direct impact on biological denitrification, with optimal activity occurring around 25–30 °C and negligible activity below 5 °C (Skiba, 2008). In order to ensure optimal biological denitrification, the reactor was placed inside a container equipped with an air conditioner, which reduced the temperature variability (30 ± 5 °C).

Furthermore, the characteristics of electro-bioremediation provide an interesting prospect for the development of decentralised water treatment. One major advantage, particularly in areas facing water scarcity, is that electro-bioremediation does not consume water in the process, and it does not generate brines, which can lead to additional contamination or require *off-site* treatment. The system only requires electricity for its operation. Thus, the coupling with renewable energy *on-site* is a matter that needs to be explored (Rovira-Alsina et al., 2021). This improvement will further enhance the sustainability, cost-effectiveness and versatility of the technology in remote areas, making it feasible to operate in locations with limited access to the electrical grid.

## 6. Conclusions

This study provides evidence for the successful transition of electro-bioremediation from a laboratory-scale to an *on-site* pilot plant, effectively bridging the gap between laboratory expectations and pilot-scale studies. Various key factors and considerations for scaling-up the technology were meticulously examined, encompassing reactor design, groundwater characteristics, and operational parameters. The achieved maximum nitrate reduction rate of 0.9 ± 0.1 kg $NO_3^-$ $m^{-3}$ $d^{-1}$ (efficiency 82 ± 18 %) was accompanied by a low energy consumption of 4.3 ± 0.4 kWh $kg^{-1}$ $NO_3^-$. Throughout the entire 3-months experimental study, the effluent water consistently met the standards for drinking water in terms of nitrate, nitrite and ammonium concentration (< 50.0 mg $NO_3^-L^{-1}$, < 0.5 mg $NO_2^-$ $L^{-1}$, and <0.5 $NH_4^+$ (European Directive 2020/2184 ). In terms of microbiome composition, *Pseudomonadaceae, Rhizobiaceae, Gallionellaceae* and *Xanthomonadaceae* were identified as the most abundant groups. Additionally, the analysis of the denitrifying biocathode revealed structural heterogeneity, with denitrification functionality mainly concentrated from the centre to the upper part of the reactor. Finally, the competitive OPEX cost of 0.40 € $m^{-3}$ encourages further investigation in this area. Future research should focus on reducing current CAPEX costs, which can be achieved through an increase in the water treatment capacity of each module. This should be done to achieve efficient treatment at an operating $HRT_{cat}$ of ≤ 0.5 h. Overall, this study provides valuable insights into the feasibility and effectiveness of electro-bioremediation as a sustainable and efficient approach to water treatment. It has established the foundations for future scaling-up electro-bioremediation, particularly *on-site* implementation.

## CRediT authorship contribution statement

**Alba Ceballos-Escalera:** Conceptualization, Data curation, Formal analysis, Investigation, Methodology, Validation, Writing – original draft. **Narcís Pous:** Conceptualization, Investigation, Methodology, Supervision, Validation, Writing – review & editing. **Lluis Bañeras:** Data curation, Formal analysis, Funding acquisition, Methodology,

Supervision, Validation, Writing – review & editing. **M. Dolors Balaguer:** Conceptualization, Funding acquisition, Supervision, Validation, Writing – review & editing. **Sebastià Puig:** Conceptualization, Funding acquisition, Supervision, Validation, Writing – review & editing.

## Declaration of competing interest

The authors declare that they have no known competing financial interests or personal relationships that could have appeared to influence the work reported in this paper.

## Data availability

Data will be made available on request.

## Acknowledgements

This work was funded through the European Union's Horizon 2020 project ELECTRA [no. 826244]. A.C-E. was supported by a PhD grant from the University of Girona (IF_UDG2020). Sebastià Puig is a Serra Hunter Fellow (UdG-AG-575) and acknowledges the funding from the ICREA Academia award. LEQUiA [2021-SGR-01352] and Ecoaqua [2021-SGR-1142] have been recognised as consolidated research groups by the Catalan Government. Open Access funding provided thanks to the CRUE-CSIC agreement with Elsevier. The authors acknowledge the technical support of Serveis Tècnics de Recerca-Universitat de Girona. Paola Chiluiza-Ramos is acknowledged for assisting in laboratory work.

## Supplementary materials

Supplementary material associated with this article can be found, in the online version, at doi:10.1016/j.watres.2024.121618.

## References

Alavijeh, H.N., Sadeghi, M., Ghahremanfard, A., 2023. Experimental and economic evaluation of nitrate removal by a nanofiltration membrane. Environ. Sci. Pollut. Res. 30, 40783–40798. https://doi.org/10.1007/s11356-022-24972-9.

Baeza, J.A., Martínez-Miró, À., Guerrero, J., Ruiz, Y., Guisasola, A., 2017. Bioelectrochemical hydrogen production from urban wastewater on a pilot scale. J. Power Sources 356, 500–509. https://doi.org/10.1016/j.jpowsour.2017.02.087.

Balch, W.E., Fox, G.E., Magrum, L.J., Woese, C.R., Wolfe, R.S., 1979. Methanogens: reevaluation of a unique biological group. Microbiol. Rev. 43, 260–296. https://doi.org/10.1128/mr.43.2.260-296.1979.

Batlle-Vilanova, P., Puig, S., Gonzalez-Olmos, R., Vilajeliu-Pons, A., Bañeras, L., Balaguer, M.D., Colprim, J., 2014. Assessment of biotic and abiotic graphite cathodes for hydrogen production in microbial electrolysis cells. Int. J. Hydrog. Energy 39, 1294–1305. https://doi.org/10.1016/j.ijhydene.2013.11.017.

Callahan, B.J., McMurdie, P.J., Rosen, M.J., Han, A.W., Johnson, A.J.A., Holmes, S.P., 2016. DADA2: high-resolution sample inference from Illumina amplicon data. Nat. Methods 13, 581–583. https://doi.org/10.1038/nmeth.3869.

Ceballos-Escalera, A., Pous, N., Balaguer, M.D., Puig, S., 2022. Electrochemical water softening as pretreatment for nitrate electro bioremediation. Sci. Total Environ. 806, 150433 https://doi.org/10.1016/J.SCITOTENV.2021.150433.

Ceballos-Escalera, A., Pous, N., Chiluiza-Ramos, P., Korth, B., Harnisch, F., Bañeras, L., Balaguer, M.D., Puig, S., 2021. Electro-bioremediation of nitrate and arsenite polluted groundwater. Water Res. 190, 116748 https://doi.org/10.1016/j.watres.2020.116748.

Cecconet, D., Devecseri, M., Callegari, A., Capodaglio, A.G., 2018. Effects of process operating conditions on the autotrophic denitrification of nitrate-contaminated groundwater using bioelectrochemical systems. Sci. Total Environ. 613–614, 663–671. https://doi.org/10.1016/j.scitotenv.2017.09.149.

Costa, A.R., de Pinho, M.N., 2006. Performance and cost estimation of nanofiltration for surface water treatment in drinking water production. Desalination 196, 55–65. https://doi.org/10.1016/J.DESAL.2005.08.030.

Dekker, A., Ter Heijne, A., Saakes, M., Hamelers, H.V.M., Buisman, C.J.N., 2009. Analysis and improvement of a scaled-up and stacked microbial fuel cell. Environ. Sci. Technol. 43, 9038–9042. https://doi.org/10.1021/ES901939R.

EEA, Zal, N., Whalley, C., Christiansen, T., 2018. European waters : assessment of status and pressures 2018, Publications Office. doi:10.2800/303664.

EurEau, 2020. Governance of Water Services in Europe. https://www.eureau.org/news/478-governance-of-water-services-in-europe. Accessed 15 Apr 2024.

Flimban, S.G.A., Ismail, I.M.I., Kim, T., Oh, S.E., 2019. Overview of recent advancements in the microbial fuel cell from fundamentals to applications: design, major elements, and scalability. Energies 12, 3390. https://doi.org/10.3390/en12173390.

Gadegaonkar, S.S., Mander, Ü., Espenberg, M., 2023. A state-of-the-art review and guidelines for enhancing nitrate removal in bio-electrochemical systems (BES). J. Water Process Eng. 53, 103788 https://doi.org/10.1016/J.JWPE.2023.103788.

García-Lledó, A., Vilar-Sanz, A., Trias, R., Hallin, S., Bañeras, L., 2011. Genetic potential for N2O emissions from the sediment of a free water surface constructed wetland. Water Res. 45, 5621–5632. https://doi.org/10.1016/j.watres.2011.08.025.

Ghosh, R., Chatterjee, S., Mandal, N.C., 2020. Stenotrophomonas, in: beneficial microbes in agro-ecology: bacteria and fungi. Acad. Press 427–442. https://doi.org/10.1016/B978-0-12-823414-3.00020-4.

Hao, R., Meng, C., Li, J., 2016. An integrated process of three-dimensional biofilm-electrode with sulfur autotrophic denitrification (3DBER-SAD) for wastewater reclamation. Appl. Microbiol. Biotechnol. 100 https://doi.org/10.1007/s00253-016-7534-4.

He, S., Tominski, C., Kappler, A., Behrens, S., Roden, E.E., 2016. Metagenomic analyses of the autotrophic Fe(II)-oxidizing, nitrate-reducing enrichment culture KS. Appl. Environ. Microbiol. 82, 2656–2668. https://doi.org/10.1128/AEM.03493-15.

Jadhav, D.A., Chendake, A.D., Vinayak, V., Atabani, A., Ali Abdelkareem, M., Chae, K.J., 2022. Scale-up of the bioelectrochemical system: strategic perspectives and normalization of performance indices. Bioresour. Technol. 363, 127935 https://doi.org/10.1016/j.biortech.2022.127935.

Jourdin, L., Sousa, J., Stralen, N.van, Strik, D.P.B.T.B., 2020. Techno-economic assessment of microbial electrosynthesis from CO2 and/or organics: an interdisciplinary roadmap towards future research and application. Appl. Energy 279, 115775. https://doi.org/10.1016/J.APENERGY.2020.115775.

Kadier, A., Chaurasia, A.K., Sapuan, S.M., Ilyas, R.A., Ma, P.C., Alabbosh, K.F.S., Rai, P. K., Logroño, W., Hamid, A.A., Hasan, H.A., 2020. Essential factors for performance improvement and the implementation of microbial electrolysis cells (MECs). in: Bioelectrochemical Systems. Springer, Singapore, pp. 139–168. https://doi.org/10.1007/978-981-15-6872-5_7.

Kim, D.U., Lee, H., Kim, H., Kim, S.G., Ka, J.O., 2016. Dongia soli sp. nov., isolated from soil from Dokdo, Korea. Antonie van Leeuwenhoek. Int. J. Gen. Mol. Microbiol. 109, 1397–1402. https://doi.org/10.1007/S10482-016-0738-X/FIGURES/3.

Kozich, J.J., Westcott, S.L., Baxter, N.T., Highlander, S.K., Schloss, P.D., 2013. Development of a dual-index sequencing strategy and curation pipeline for analyzing amplicon sequence data on the miseq illumina sequencing platform. Appl. Environ. Microbiol. 79, 5112–5120. https://doi.org/10.1128/AEM.01043-13.

Labbé, N., Parent, S., Villemur, R., 2003. Addition of trace metals increases denitrification rate in closed marine systems. Water Res. 37, 914–920. https://doi.org/10.1016/S0043-1354(02)00383-4.

Lai, A., Aulenta, F., Mingazzini, M., Palumbo, M.T., Papini, M.P., Verdini, R., Majone, M., 2017. Bioelectrochemical approach for reductive and oxidative dechlorination of chlorinated aliphatic hydrocarbons (CAHs). Chemosphere. https://doi.org/10.1016/j.chemosphere.2016.11.072.

Lust, R., Nerut, J., Kasak, K., Mander, Ü., 2020. Enhancing nitrate removal fromwaters with low organic carbon concentration using a bioelectrochemical system-a pilot-scale study. Water 12, 516. https://doi.org/10.3390/w12020516.

Lycus, P., Bøthun, K.L., Bergaust, L., Shapleigh, J.P., Bakken, L.R., Frostegård, Å., 2017. Phenotypic and genotypic richness of denitrifiers revealed by a novel isolation strategy. ISME J. 11, 2219–2232. https://doi.org/10.1038/ismej.2017.82.

Papillon, J., Ondel, O., Maire, É., 2021. Scale up of single-chamber microbial fuel cells with stainless steel 3D anode: effect of electrode surface areas and electrode spacing. Bioresour. Technol. Rep. 13, 100632 https://doi.org/10.1016/J.BITEB.2021.100632.

Peter-Varbanets, M., Zurbrügg, C., Swartz, C., Pronk, W., 2009. Decentralized systems for potable water and the potential of membrane technology. Water Res 43, 245–265. https://doi.org/10.1016/j.watres.2008.10.030.

Pous, N., Balaguer, M.D., Colprim, J., Puig, S., 2018. Opportunities for groundwater microbial electro-remediation. Microb. Biotechnol. 11, 119–135. https://doi.org/10.1111/1751-7915.12866.

Pous, N., Puig, S., Balaguer, M.D., Colprim, J., 2017. Effect of hydraulic retention time and substrate availability in denitrifying bioelectrochemical systems. Environ. Sci. Water Res. Technol. 3, 922–929. https://doi.org/10.1039/c7ew00145b.

Pous, N., Puig, S., Dolors Balaguer, M., Colprim, J., 2015. Cathode potential and anode electron donor evaluation for a suitable treatment of nitrate-contaminated groundwater in bioelectrochemical systems. Chem. Eng. J. 263, 151–159. https://doi.org/10.1016/j.cej.2014.11.002.

Puig, S., Coma, M., Desloover, J., Boon, N., Colprim, J., Balaguer, M.D., 2012. Autotrophic denitrification in microbial fuel cells treating low ionic strength waters. Environ. Sci. Technol. 46, 2309–2315. https://doi.org/10.1021/es2030609.

Quejigo, J.R., Korth, B., Kuchenbuch, A., Harnisch, F., 2021. Redox potential heterogeneity in fixed-bed electrodes leads to microbial stratification and inhomogeneous performance. ChemSusChem 14, 1155–1165. https://doi.org/10.1002/cssc.202002611.

Rezvani, F., Sarrafzadeh, M.H., Ebrahimi, S., Oh, H.M., 2019. Nitrate removal from drinking water with a focus on biological methods: a review. Environ. Sci. Pollut. Res. 26, 1124–1141. https://doi.org/10.1007/s11356-017-9185-0.

Rivett, M.O., Buss, S.R., Morgan, P., Smith, J.W.N., Bemment, C.D., 2008. Nitrate attenuation in groundwater: a review of biogeochemical controlling processes. Water Res. 42, 4215–4232. https://doi.org/10.1016/j.watres.2008.07.020.

Rossi, R., Logan, B.E., 2022. Impact of reactor configuration on pilot-scale microbial fuel cell performance. Water Res. 225, 119179 https://doi.org/10.1016/J.WATRES.2022.119179.

Rovira-Alsina, L., Balaguer, M.D., Puig, S., 2021. Thermophilic bio-electro carbon dioxide recycling harnessing renewable energy surplus. Bioresour. Technol. 321, 124423 https://doi.org/10.1016/J.BIORTECH.2020.124423.

Schröder, U., Harnisch, F., Angenent, L.T., 2015. Microbial electrochemistry and technology: terminology and classification. Energy Environ. Sci. 8, 513–519. https://doi.org/10.1039/c4ee03359k.

Skiba, U., Jørgensen, S.E., Fath, B.D., 2008. Denitrification. Encyclopedia of Ecology. Academic Press, Oxford, pp. 866–871. https://doi.org/10.1016/B978-008045405-4.00264-0.

Solera, J.S., Castaño, M.J., 2008. Brucellosis, in: international encyclopedia of public health. Acad. Press 357–369. https://doi.org/10.1016/B978-012373960-5.00560-8.

Twomey, K.M., Stillwell, A.S., Webber, M.E., 2010. The unintended energy impacts of increased nitrate contamination from biofuels production. J. Environ. Monit. 12, 218–224. https://doi.org/10.1039/b913137j.

U.N. Water, 2021. Summary Progress Update 2021 – SDG 6 – water and sanitation for all. Version: July 2021. Geneva, Switzerland.

Vilar-Sanz, A., Pous, N., Puig, S., Balaguer, M.D., Colprim, J., Bañeras, L., 2018. Denitrifying nirK-containing alphaproteobacteria exhibit different electrode driven nitrite reduction capacities. Bioelectrochemistry 121, 74–83. https://doi.org/10.1016/j.bioelechem.2018.01.007.

Vilar-Sanz, A., Puig, S., García-Lledó, A., Trias, R., Balaguer, M.D., Colprim, J., Bañeras, L., 2013. Denitrifying bacterial communities affect current production and nitrous oxide accumulation in a microbial fuel cell. PLoS One 8, e63460. https://doi.org/10.1371/journal.pone.0063460.

Wang, X., Aulenta, F., Puig, S., Esteve-Núñez, A., He, Y., Mu, Y., Rabaey, K., 2020. Microbial electrochemistry for bioremediation. Environ. Sci. Ecotechnol. 1, 100013 https://doi.org/10.1016/j.ese.2020.100013.

WHO and UNICEF, 2021 Progress on household drinking water, sanitation and hygiene 2000-2020: five years into the SDGs. Geneva: World Health Organization (WHO) and the United Nations Children's Fund (UNICEF), 2021. Licence: CC BY-NC-SA 3.0 IGO.

Wrighton, K.C., Virdis, B., Clauwaert, P., Read, S.T., Daly, R.A., Boon, N., Piceno, Y., Andersen, G.L., Coates, J.D., Rabaey, K., 2010. Bacterial community structure corresponds to performance during cathodic nitrate reduction. ISME J. 4, 1443–1455. https://doi.org/10.1038/ismej.2010.66.

Xin, J., Wang, Y., Shen, Z., Liu, Y., Wang, H., Zheng, X., 2021. Critical review of measures and decision support tools for groundwater nitrate management: a surface-to-groundwater profile perspective. J. Hydrol. 598, 126386 https://doi.org/10.1016/J.JHYDROL.2021.126386.

Zhang, D., Liu, Y., Han, Y., Zhang, Y., Jia, X., Li, W., Li, D., Jing, L., 2021. Nitrate removal from low C/N wastewater at low temperature by immobilized Pseudomonas sp. Y39-6 with versatile nitrate metabolism pathways. Bioresour. Technol. 326, 124794 https://doi.org/10.1016/J.BIORTECH.2021.124794.

Zhao, F., Xin, J., Yuan, M., Wang, L., Wang, X., 2022. A critical review of existing mechanisms and strategies to enhance N2 selectivity in groundwater nitrate reduction. Water Res. 209, 117889 https://doi.org/10.1016/j.watres.2021.117889.

Zhong, L., Yang, S.S., Ding, J., Wang, G.Y., Chen, C.X., Xie, G.J., Xu, W., Yuan, F., Ren, N. Q., 2021. Enhanced nitrogen removal in an electrochemically coupled biochar-amended constructed wetland microcosms: the interactive effects of biochar and electrochemistry. Sci. Total Environ. 789, 147761 https://doi.org/10.1016/J.SCITOTENV.2021.147761.